

## Local Density Fluctuations of Moving Vortices in the Solid and Liquid Phases in $\text{Bi}_2\text{Sr}_2\text{CaCu}_2\text{O}_y$

T. Tsuboi, T. Hanaguri, and A. Maeda

*Department of Basic Science, The University of Tokyo, 3-8-1 Komaba, Meguro-ku, Tokyo 153, Japan*

(Received 18 August 1997)

By a new method using a 2DEG micro-Hall probe, the local field noise generated by current-driven vortices was investigated around the vortex melting transition field  $H_m$  in  $\text{Bi}_2\text{Sr}_2\text{CaCu}_2\text{O}_y$ . A broad-band noise (BBN) was found to occur just when the pinned vortices start moving. When the vortex velocity increased, the BBN disappeared. In turn, a narrow-band noise appeared. These noises were observed in the liquid phase as well as in the solid phase. We conclude that in  $\text{Bi}_2\text{Sr}_2\text{CaCu}_2\text{O}_y$  the moving vortices in the solid and liquid phases fluctuate qualitatively in the same manner near  $H_m$ . This is a characteristic of the vortices in  $\text{Bi}_2\text{Sr}_2\text{CaCu}_2\text{O}_y$ . [S0031-9007(98)06160-2]

PACS numbers: 74.60.Ge, 74.25.Bt, 74.25.Fy, 74.72.Hs

Recent experiments have successfully identified the first-order melting transition of vortices in high-temperature superconductors [1,2]. While theoretical studies on this transition have been done mainly in the clean system [3,4], pinning is important in real systems. Resistive behavior suggests that the pinning is affected by the transition. In the case of  $\text{YBa}_2\text{Cu}_3\text{O}_x$ , only the solid phase is pinned, whereas vortex liquid shows a simple Bardeen-Stephen-type flux-flow behavior [5]. The drastic change of effectiveness of pinning at the transition results in a sharp drop in resistivity. On the other hand, in  $\text{Bi}_2\text{Sr}_2\text{CaCu}_2\text{O}_y$  we found previously that resistivity shows a more complex behavior [6]. Nonlinear resistivity was observed both below and above the melting transition field, and at higher fields resistivity showed thermally assisted-flux-flow-like behavior. This behavior which is very different from the case of  $\text{YBa}_2\text{Cu}_3\text{O}_x$  indicates that the liquid vortices are pinned in  $\text{Bi}_2\text{Sr}_2\text{CaCu}_2\text{O}_y$ , while the mechanism of pinning can be quite different in the solid and liquid phases [7]. These findings strongly suggest the complicated relationship between the pinning and the vortex phase. Thus, further experimental investigations are still needed. Besides, the dynamic properties of the current-driven vortices under the influence of pinning become stimulating, since new concepts such as "dynamic melting" have been proposed recently [8]. Therefore, studies on the dynamic properties of the weakly pinned vortices are highly requested to investigate both the quasistatic and dynamic nature of the real vortex system.

Noise measurement has proved to be a powerful tool for this purpose [9]. However, no noise measurement was performed in  $\text{Bi}_2\text{Sr}_2\text{CaCu}_2\text{O}_y$  around the vortex melting transition, which contrasts with the case of  $\text{YBa}_2\text{Cu}_3\text{O}_x$  where a few experiments have been reported [10,11]. The main reason is considered to be a problem of sensitivity. Most of the noise studies performed so far measured voltage noise. However, in the case of  $\text{Bi}_2\text{Sr}_2\text{CaCu}_2\text{O}_y$ , resistivity just above the transition is the order of  $10^{-7} \Omega \text{ cm}$ , 2 orders of magnitude smaller than that of  $\text{YBa}_2\text{Cu}_3\text{O}_x$ .

This makes ordinary voltage-noise measurement quite difficult. As will be presented below, we developed a novel method which detects fluctuations of local field or vortex density with a sensitivity as high as  $0.001 \text{ G/Hz}^{1/2}$ . By using this method, we observed the noise generated by the current-driven vortices both below and above the vortex melting transition in  $\text{Bi}_2\text{Sr}_2\text{CaCu}_2\text{O}_y$  for the first time. There were two characteristic types of noise appearing only when the current was flown. One of them was a broad-band noise (BBN), of which appearance corresponded to the apparent onset of resistivity. It directly means that the BBN is generated by the pinned vortices which start moving by Lorentz force. Moreover, the power spectral density of BBN was  $1/f$ -like at an earlier stage, then changed into a Lorentzian for higher velocities. Around this crossover, the intensity of BBN took maximum. The other noise was a sharp peak in the spectrum, namely, a narrow-band noise (NBN). It appeared around the crossover region mentioned just above, and shifted to higher frequencies as the vortex velocity increased. The frequency of NBN was found to scale with the inverse of transit time. In the smaller-velocity region where only  $1/f$ -like BBN was observed, it was found that bulk pinning plays an important role on the vortex motion, such as in the so-called plastic flow state visualized by recent numerical simulations [12]. In the larger-velocity region where both Lorentzian BBN and NBN coexist, surface pinning seems to become significant in place of bulk pinning. The most important finding is that these features are common both in the solid and liquid phases near the melting transition field  $H_m$ . Similarity of solid and liquid vortices in dynamic behavior near  $H_m$  is considered to be characteristic of the vortex system in  $\text{Bi}_2\text{Sr}_2\text{CaCu}_2\text{O}_y$ .

A single crystal of  $\text{Bi}_2\text{Sr}_2\text{CaCu}_2\text{O}_y$  was grown by the floating-zone method and annealed to have an optimal oxygen content. The detailed procedure on sample preparation was described elsewhere [6]. The superconducting transition temperature  $T_c$  defined as zero resistivity temperature was 88 K. The dimensions of the sample were

$1 \times 0.4 \times 0.02 \text{ mm}^3$ . The sample was directly placed on a 2DEG micro-Hall probe, of which the active area was  $5 \times 5 \mu\text{m}^2$ . This area was located far from the electrical contacts as well as any edges of the sample. Hall voltage was first magnified 100 times by an NF LI-75A low-noise preamplifier and fed into an HP-35665A fast-Fourier transform analyzer. Frequency range was taken from 1 to 400 Hz. The electrical grounding was carefully taken and the signals were averaged typically for 500 times. Then the background noise level was as low as  $0.001 \text{ G/Hz}^{1/2}$  except at lowest frequencies. Data were collected for various magnetic fields and currents around the vortex melting transition. Magnetic fields were applied perpendicular to the  $\text{CuO}_2$  plane, while currents were within the plane.

Figure 1 shows the frequency spectra at 80 K for various fields with and without the applied current. When no current was applied, as is shown in the upper panel, only the environmental background noise was seen for each applied field. In contrast, under the finite current flow,

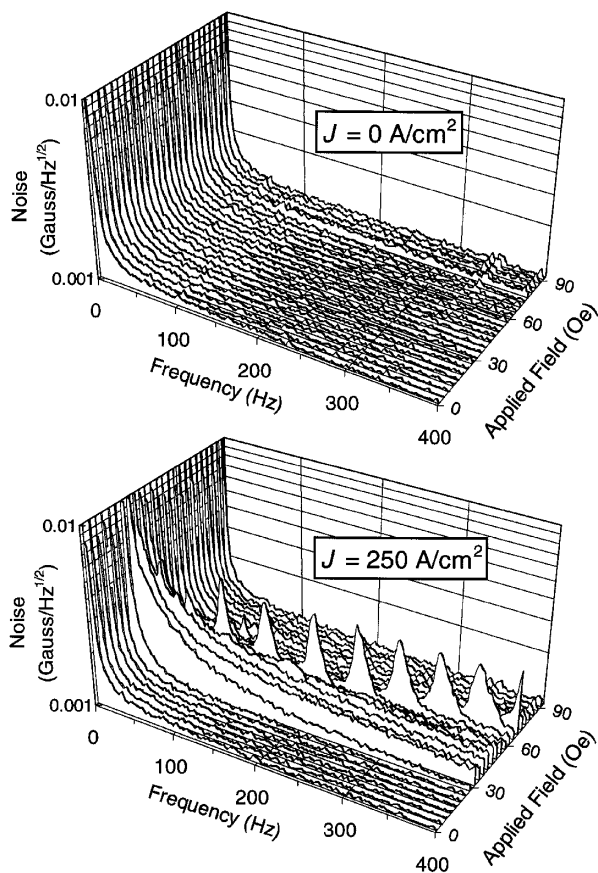


FIG. 1. Local-field noise spectrum as a function of applied field at 80 K in  $\text{Bi}_2\text{Sr}_2\text{CaCu}_2\text{O}_y$ , for the current densities  $J = 0 \text{ A/cm}^2$  (the upper panel) and  $J = 250 \text{ A/cm}^2$  (the lower panel). For  $J = 0 \text{ A/cm}^2$ , only the background noise is observed in the entire region. For  $J = 250 \text{ A/cm}^2$ , there appear the prominent noises, a broad-band noise and a narrow-band noise.

the prominent noise came out. The same spectral shapes were found for four independent field sweeps, two of which were in the field-increasing process from the zero-field cooled state, and the other two were in the field-decreasing process. One can distinguish two characteristic types of noise at a glance. One of them was a broad-band noise. For the current density  $J = 250 \text{ A/cm}^2$ , it appeared about 20 Oe and its intensity increased to reach a maximum around 30 Oe. With further increasing field, it decreased, and disappeared around 45 Oe. Where the intensity of BBN took maximum, there appeared another component in the spectrum, a peak structure, namely, a narrow-band noise. The frequency of NBN shifted to higher frequencies as the field increased. Between 30 and 45 Oe, both BBN and NBN were observed.

In Fig. 2, we show the field dependence of the intensity of BBN, together with the resistivity and the local magnetization of the same sample. As is clearly seen, the BBN was observed just around the apparent onset of resistivity. In other words, BBN appears when the pinned vortices get out of the stationary state into the moving state. For larger current densities, these take place far below the vortex melting transition field  $H_m$  defined as a step in magnetization. On the other hand, for the smallest current, the onset of resistivity was just at  $H_m$ , and the BBN was observed even above  $H_m$ . Namely, BBN appeared in the vortex liquid phase near  $H_m$ . There seems to be no discontinuous change at  $H_m$ .

As shown in Fig. 3, we plotted the NBN frequency as a function of applied field for different current densities. Also shown is the inverse of the transit time, which is given by  $v/w$ , where  $v$  is the vortex velocity, and  $w$  is the width of the sample. The velocity  $v$  was calculated using the equation  $E = B \times v/c$ , where  $E$  is the electric field appearing along the current direction, which is the quantity directly measured in “resistivity” measurement,  $B$  is the field density, and  $c$  is the speed of light. The qualitative and even quantitative correspondence of the NBN frequency to the value  $w/v$  strongly suggests that this noise is related to the entry and exit of the vortices to/from the sample. As for the spectral shape of NBN, no discontinuous change was found at  $H_m$ .

It is likely that pinning plays a crucial role on the generation of the noises including both BBN and NBN, since they appear near the resistivity onset. However, it has not been established what kind of pinning operates. First of all, it is to be clarified which pinning is more important: bulk or surface. Recently, using the array of a number of micro-Hall probes, we have confirmed directly that BBN is attributed to bulk pinning, while NBN to surface pinning. The detailed results will be published elsewhere. Here, we summarize only three main points: (i) BBN was generated everywhere on the sample, and the intensity of it was smaller near the edge. (ii) Although BBN was  $1/f$ -like or Lorentzian, BBN had a *site-specific* shape. This “fingerprint” effect was

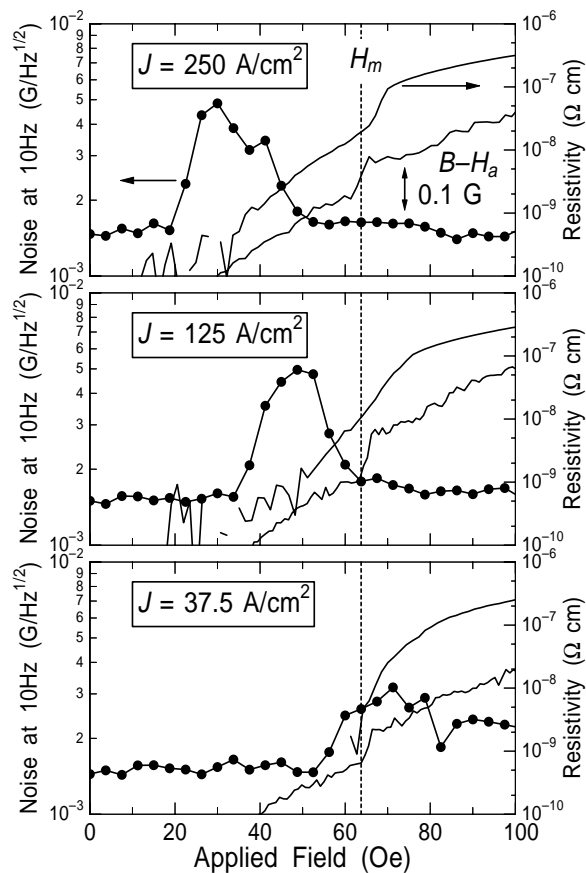


FIG. 2. The intensity of the spectrum at 10 Hz, the resistivity, and the local magnetization of the sample are plotted as a function of applied field at 80 K. Local magnetization is given by  $B - H_a$ , where  $B$  is local-field density and  $H_a$  is applied field. Only the relative scale of it was shown in the top panel as an arrow. The vortex melting transition field  $H_m$  is defined as a step in magnetization. The intensity at 10 Hz, which represents that of BBN, is highly enhanced around the apparent onset of resistivity. It is to be noted that for  $J = 37.5 \text{ A/cm}^2$ , the enhancement occurs at and above  $H_m$ .

prominent when the vortex velocity was smaller. (iii) BBN was invariant under the current reversal, while NBN changed. If surface pinning generates BBN, the intensity would become larger as one gets closer to the edge of the sample. However, we obtained the opposite result. Other than this, BBN was site specific and current invariant. It is to be noted that the observing sites are located side by side only in the interval of  $50 \mu\text{m}$ . Therefore, if the fluctuations are created at one side and penetrate the sample, the spectral shape should be similar rather than site specific. In addition, in such a case, the noise would change under the current reversal, since the vortex-entering side where the fluctuations are supposed to be generated is changed. That is not the case for BBN, and rather the case for NBN. We can conclude that BBN is characterized by the conditions existing within the local site, and that NBN is characterized by some large-scale conditions. More directly, BBN is related to the local

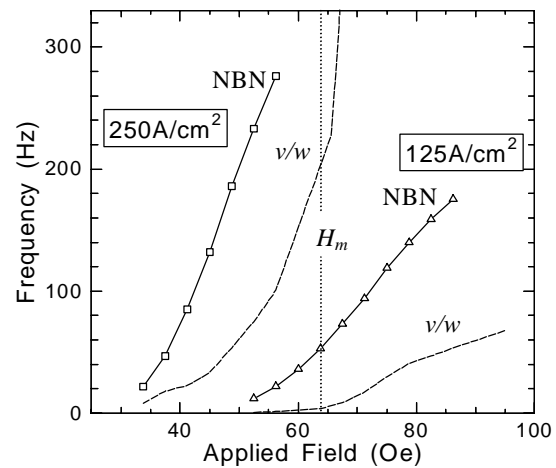


FIG. 3. Plot of the center frequency of NBN vs applied field. Also shown is the inverse of the transit time, which is given by  $v/w$ , where  $v$  is the vortex velocity and  $w$  is the width of the sample. These two curves are scaled well for each current density.

specific distribution of pinning centers. As for NBN, it seems to be related to surface pinning, if one takes account of the correspondence of NBN frequency to the transit frequency  $w/v$ .

Back to the main results, it was found that the noises including both BBN and NBN were controlled by the vortex velocity and not by the thermodynamic phase. Vortex-motion-induced noises were observed in several materials [10,11,13–15]. For the smaller-velocity region, various features were reported.  $1/f$  noise was observed in Ref. [13]. Non-Gaussian noise [14,15] and other kinds of noise [10,11] were also observed. On the other hand, for the larger-velocity region, a Lorentzian was observed rather commonly. As for our data, the power spectral density of BBN was found to be  $1/f$  at first, and then changed into a Lorentzian. This crossover region took place around where the intensity of BBN took maximum. Compared with the previous works for other materials, it is reasonable that the  $1/f$ -noise region corresponds to the smaller-velocity region, and the Lorentzian-noise region to the larger-velocity one. We propose that these two regions are qualitatively different from each other. In the larger-velocity region, as the velocity increases, the intensity of BBN decreases gradually, which means in general that the size of a kind of vortex bundle which consists of a noise source unit gradually shrinks. This transient state continues to the ordered “quiet” flux flow with no noise as the vortex velocity increases more. In addition, NBN appeared in this region. As was discussed above, NBN is attributed to surface pinning. Transmission of such a surface effect over the whole sample becomes possible only on the condition that bulk pinning is ineffective. Taking all these into account, we conclude that in the larger-velocity region bulk pinning becomes gradually ineffective and that, in turn, surface pinning dominates

the vortex dynamics. On the other hand, in the smaller-velocity region, bulk pinning should be crucial, because only  $1/f$ -like BBN was observed, and moreover a site-specific feature was prominent. In the simple analysis,  $1/f$  noise has been modeled by a summation of many Lorentzians with widely distributed roll-off frequencies. We consider these fluctuations to exist in the area monitored by us which contains about  $10 \times 10$  vortices. Temporal appearance, disappearance, and interchange of filamentary vortex-flow channels in this scale can be the origin of such a noise. The similar picture was provided by recent simulations [12], which describe the so-called plastic flow.

Finally, it should be stressed that these noises were observed both in the solid and liquid phases. We found that these noises are controlled by the velocity of vortices and that there is no qualitative change at  $H_m$ . It demonstrates that at least near  $H_m$  the moving vortices in the liquid phase are fluctuated qualitatively in the same manner as are in the solid phase. At first, they are under the influence of bulk pinning. As the velocity increases, the surface effect is considered to be more important. This is very different from the case of  $\text{YBa}_2\text{Cu}_3\text{O}_x$  [10,11], where the noises corresponding to BBN and NBN were observed only in the solid phase. We consider that the similarity of the dynamic properties between the solid and liquid phases is characteristic of vortices in  $\text{Bi}_2\text{Sr}_2\text{CaCu}_2\text{O}_y$ . Previously in  $\text{Bi}_2\text{Sr}_2\text{CaCu}_2\text{O}_y$  [6], we proposed that the pinning of liquid becomes outstanding as the vortices become sparse, because relative pin density becomes large. As a result, pinning is expected to compete with the decreasing vortex-vortex interaction. According to this scenario, pinning of the vortex liquid in  $\text{Bi}_2\text{Sr}_2\text{CaCu}_2\text{O}_y$  can be attributed to the fact that in  $\text{Bi}_2\text{Sr}_2\text{CaCu}_2\text{O}_y$  the melting transition field is much lower than that of  $\text{YBa}_2\text{Cu}_3\text{O}_x$  due to large anisotropy.

In conclusion, we investigated the noise in the local density of vortices around the vortex phase transition in  $\text{Bi}_2\text{Sr}_2\text{CaCu}_2\text{O}_y$  by a new method using a 2DEG micro-Hall probe. Two characteristic types of noise, a broad-band noise and a narrow-band noise were observed both in the solid and liquid phases only when the current was flown. The appearance of BBN corresponds to the apparent onset of resistivity. It demonstrates that the BBN occurs just when the vortex system changes from the stationary pinned state into a moving state under the effect of pinning. We found that in the smaller-velocity region the vortices are fluctuated due to bulk pinning, and pointed out the consistency of this picture with the so-called plastic flow state. When the vortex velocity

increases, BBN turned from  $1/f$ -like into Lorentzian, and NBN appeared. At the same time, the intensity of BBN gradually decreased. In this region, surface pinning seems to become crucial for the fluctuations. The most important point in this paper is that these features are observed both in the solid and liquid phases near  $H_m$ . We conclude that in  $\text{Bi}_2\text{Sr}_2\text{CaCu}_2\text{O}_y$  both the solid and liquid vortices in motion are fluctuated qualitatively in the same manner at least near  $H_m$ . That is, they are under the influence of bulk pinning at the first stage, and then a surface effect becomes significant with increasing the velocity. A similar behavior between the solid and liquid vortices near  $H_m$  is considered to be characteristic of the vortices in  $\text{Bi}_2\text{Sr}_2\text{CaCu}_2\text{O}_y$ .

The authors are grateful to Y. Kawaguchi, H. Hirai, and S. Komiyama for technical assistance in preparing the Hall probes, and to H. Yasuda and Y. Tsuchiya for assistance with the crystal growth. They acknowledge D.G. Steel for helpful discussions and critical readings of the manuscript. This work was supported by the Grant-in-Aid for Scientific Research from the Ministry of Education, Science, Sports and Culture of Japan.

- 
- [1] H. Pastoriza *et al.*, Phys. Rev. Lett. **72**, 2951 (1994); Y. Yamaguchi *et al.*, Physica (Amsterdam) **246C**, 216 (1995); E. Zeldov *et al.*, Nature (London) **375**, 373 (1995); T. Hanaguri *et al.*, Physica (Amsterdam) **256C**, 111 (1996).
  - [2] R. Liang *et al.*, Phys. Rev. Lett. **76**, 835 (1996); U. Welp *et al.*, Phys. Rev. Lett. **76**, 4809 (1996); A. Schilling *et al.*, Nature (London) **382**, 791 (1996).
  - [3] G. Blatter *et al.*, Rev. Mod. Phys. **66**, 1125 (1994).
  - [4] A. Houghton *et al.*, Phys. Rev. B **40**, 6763 (1989).
  - [5] H. Safar *et al.*, Phys. Rev. Lett. **69**, 824 (1992); J.A. Fendrich *et al.*, Phys. Rev. Lett. **77**, 2073 (1996).
  - [6] T. Tsuboi *et al.*, Phys. Rev. B **55**, R8709 (1997).
  - [7] V.M. Vinokur *et al.*, Phys. Rev. Lett. **65**, 259 (1990).
  - [8] A.E. Koshelev and V.M. Vinokur, Phys. Rev. Lett. **77**, 2073 (1996).
  - [9] J.R. Clem, Phys. Rep. **75**, 1 (1981).
  - [10] H. Safar *et al.*, Phys. Rev. B **52**, 6211 (1995).
  - [11] G. D'Anna *et al.*, Phys. Rev. Lett. **75**, 3521 (1995).
  - [12] C.J. Olson *et al.*, e-print cond-mat/9612078; F. Nori, Science **271**, 1373 (1996).
  - [13] W.J. Yeh and Y.H. Kao, Phys. Rev. B **44**, 360 (1991); W.J. Yeh *et al.*, Physica (Amsterdam) **195C**, 367 (1992).
  - [14] S. Bhattacharya and M.J. Higgins, Phys. Rev. Lett. **70**, 2617 (1993); A.C. Marley *et al.*, Phys. Rev. Lett. **74**, 3029 (1995).
  - [15] R.D. Merithew *et al.*, Phys. Rev. Lett. **77**, 3197 (1996).